Operando and high-throughput multiscale-tomography

Rau, Christoph, Marathe, Shashidhara, Bodey, Andrew, Storm, Malte, Batey, Darren, et al.

Christoph Rau, Shashidhara Marathe, Andrew J. Bodey, Malte Storm, Darren Batey, Silvia Cipiccia, Peng Li, Ralf Ziesche, "Operando and high-throughput multiscale-tomography," Proc. SPIE 11840, Developments in X-Ray Tomography XIII, 118401E (15 October 2021); doi: 10.1117/12.2598470

SPIE.

Event: SPIE Optical Engineering + Applications, 2021, San Diego, California, United States

Operando and High-throughput multicscale-tomography

C. Rau*[a,b,c], S. Marathe[a], A.J. Bodey[a], M. Storm[a,d], D. Batey[a], S. Cipiccia[a,e], P. Li[a], R. Ziesche[a], M. Al-Hada[a,f,g], S.L.M. Schroeder[a,h,i], G. Das[a,h,i], A. Goswami[j].

[a]Diamond Light Source Ltd, Harwell Science and Innovation Campus, Didcot, OX 11 0DE, UK
[b]University of Manchester, School of Materials Grosvenor St., Manchester, M1 7HS, UK
[c]Northwestern University, 303 E. Chicago Avenue, Chicago, IL 60611-3008, USA
[d]Institute of Materials Physics, Helmholtz-Zentrum hereon, Max-Planck-Str. 1, Geesthacht, 21502, Germany
[e]Department Medical Physics and Biomedical Engineering, University College London, London WC1E 6BT, UK
[f]Department of Chemical Engineering, University College London, London, WC1E 7JE, UK
[g]The Faraday Institution, Quad One, Harwell Science and Innovation Campus, Didcot, OX11 0RA, UK
[h]School of Chemical and Process Engineering, University of Leeds, Leeds, LS2 9JT
[i]Continuous Manufacturing and Crystallisation Group, Research Complex at Harwell, Harwell Science and Innovation Campus, Didcot, OX 11 0DE, UK
[j]Department of Life Sciences, The Natural History Museum, London, UK

ABSTRACT

We report about the current and future multi-scale imaging capabilities at the Diamond beamline I13L. Operando and high-throughput imaging is achieved by using either the so-called pink-beam or a multilayer monochromator. The beam modes are compatible with the different techniques covering the micro- to the nano-length scale. In-line phase contrast tomography with up to 300 samples per day is achieved when using an automated sample changer. Fast recording (without the sample changing robot) enables operando studies with a vast variety of dedicated sample environments. For imaging with highest spatial resolution we managed to improve significantly the recording speed of ptycho-tomography, which is now in the order of hours. The Diamond II upgrade planned for 2027 will close the gap in recording times for real and reciprocal space imaging, permitting operando imaging across all length scales. The beamline covers a large range of scientific areas such as materials science, biology and medical research, environmental sciences.

Keywords: tomography, synchrotron radiation, nano-imaging, phase contrast, X-ray microscopy, ptychography, Bragg-CDI, pink-beam, operando imaging, high-throughput imaging

1. INTRODUCTION

Over the last years the Diamond beamline I13L addressed science in the areas of bio-systems and -materials, materials science and environmental sciences/geophysics to name some areas. The research focuses on systems under dynamic conditions, evolving over time. For example the charging/discharging of batteries, loading sandstone/brine mix with CO_2[1], corrosion of steel[2], or the movement of mouse knees under load[3], biomass pyrolyses[4], or the degradation of tooth enamel[5] have been studied. The temporal evolution of these systems is typically observed over the timescale of hours, and probed with scans in the range of minutes or faster. Up to recently most of the investigations have been carried out on the micrometer length scale, with increasing research on smaller length scales[6]. By improving the experimental capabilities, namely the use of pink-beam and a broadband multilayer monochromator, recording times become comparable across the length scales covered at I13L.

Developments in X-Ray Tomography XIII, edited by Bert Müller
Ge Wang, Proc. of SPIE Vol. 11840, 118401E · © 2021 SPIE
CCC code: 0277-786X/21/$21 · doi: 10.1117/12.2598470

We expanded most recently our capabilities for high-throughput data acquisition by the installation of robotic sample changer. This project aims for measuring large numbers of *static* samples and will be beneficial in biological applications, such as for biodiversity or study of bone formation. For materials sciences, sample series can be explored by changing multiple parameters such as composition, preparation condition and repeat measurements become feasible within reasonable timescales. Some topics will require a significant increase of capacities –especially in terms of data analyses-, which will be addressed latest with the Diamond II upgrade.

2. THE BEAMLINE

Diamond is a 3 GeV third generation storage ring for synchrotron radiation. The I13L beamline is located in one of the long straight sections, which is divided into two shorter sections. This so-called 'mini-beta' layout permits the independent operation of two branchlines with small gaps of the undulator sources (5mm and 6.15mm). The beamline operates in the 6-30keV photon energy range with resolution from the micro- to the nano-range. The Diamond-Manchester imaging branchline provides micrometer to 100nm resolution with real space imaging, the coherence branch is designed for imaging with highest resolution using techniques in reciprocal space such as ptychography and Bragg-CDI, see figure 1[7, 8]. The current performance of the different techniques is listed in table 1. Each branchline is equipped with a series of slits, X-ray filters, horizontal deflecting mirrors and Si(111) monochromators. The Diamond-Manchester Imaging Branchline also operates with a multilayer monochromator, with different sets of multilayer stripes. On the Coherence Branchline the lateral coherence length can be adapted with front-end slits and a CRL focusing optic located in the first optics hutch.

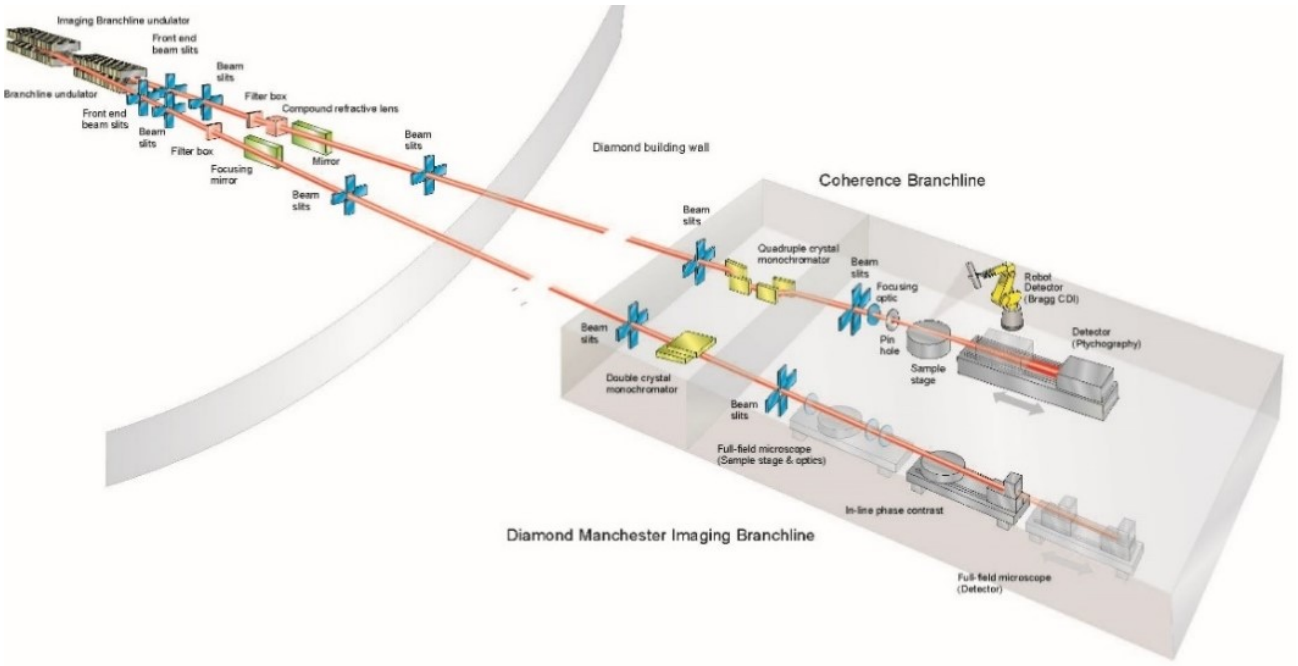

Figure 1: Schematic overview of the I13L beamline and its endstations.

Table 1: Imaging methods available at the Diamond beamline I13L.

Method	Micro-tomography	Grating interferometry	Full-field microscopy	Ptychography	Bragg-CDI
Branchline		Imaging		Coherence	
Resolution	1-8 µm	>5 µm & SAXS	50-100nm	30-100nm	TBD
Field of view*	1-14 mm	1-14 mm	50-100 µm	<300 µm	<10µm
Energy range	8-30keV	14-25keV	8-13keV	6-20keV	6-20keV
t_{exp}	100µs-100ms	50-100ms	~100ms	10µs-100ms[2)]	sec.-min.
$t_{Tomo\ scan}$	sec.-min.	sec.-min.	sec.-min.	~6h	~5h
Pink/MLM	Pink	Pink/MLM	MLM	DCM	DCM
Element spec.	Yes	Not tested	Not tested	Yes	-
Spectroscopy	-	-	-	Yes	-

2.1. Pink beam and multilayer monochromator

The use of the so-called 'pink beam' or alternatively multilayer increases the photon flux by up to two orders of magnitude, compared to when using a Si(111) monochromator. We investigated the impact of the broadband illumination on the image quality for the different techniques (in-line phase contrast, grating interferometry, full-field microscopy) used on the imaging branchline in particular[9-11].

The radiation of the beamline is generated by undulators. They produce a discontinuous spectrum of X-rays, characterized by intensity peaks at specific photon energies, called harmonics (see figure 2, faint yellow line). Each undulator harmonic has a bandwidth of a few percent. Few harmonics can be filtered out by a band-pass combination of X-ray filters (high pass) and a reflecting X-ray mirror (low pass)[12], see figure 2 left. Typical materials used are carbon and aluminum for broadband filtering, or silver. Alternatively, a multilayer monochromator with varying bandwidths between 0.5% and 5% can be used. The multilayer system consists of a couple of hundred alternating high/low refractive index materials (here: Mo, V, Ru alternating with B_4C, figure 2 right) determining energy range and bandwidth (for study on properties see[13, 14]).

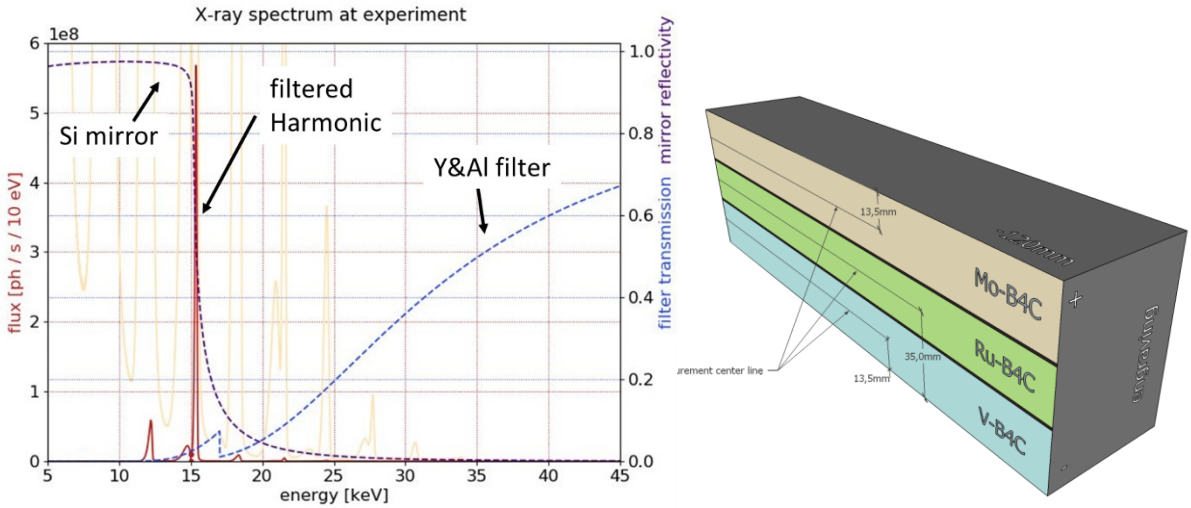

Figure 2: left: Pink-beam spectrum calculation for I13 imaging branchline (simulation M. Storm), undulator spectrum in yellow, transmitted harmonic in red, mirror reflectivity in purple, filter transmission in blue; right: scheme of multilayer systems used for multilayer monochromator, with a bandwidths between 0.5% and 5%.

It turns out that pink beam is compatible for in-line phase contrast imaging and grating interferometry, while for full-field microscope the multilayer monochromator can be used[15]. This is essential and core for the rapid data acquisition.

3. EXPERIMENTS

3.1.1 High throughput micro-tomography

The micro-tomography setup is located on the I13-2 Diamond-Manchester Imaging Branchline, consisting of a high-precision rotation stage and a visible light detector using an X-ray to visible light converting scintillation screen coupled to a visible light microscope. Most experiments are carried out in pink-beam mode, with a minimal ID gap of 5mm, a set of filters (typically 1.3mm glassy carbon, 3mm aluminium and for higher photon energies either 100 μm steel or palladium and silver filters) and either the silicon, platinum or rhodium strip of the horizontally deflecting mirror. The distance between sample and detector can be increased to up to about 2 meters for in-line phase contrast imaging, suitable for investigating unstained soft biological tissues[16]. Typical scanning times are in the range of minutes.

Most recently a sample changing system has been added to the setup (see figure 3, left). The system consists of a robotic arm, a plate for intermediate storage of the samples and a (cryo-compatible) sample gripper. The current version of the gripper can handle samples with up to 5mm diameter. Samples are identified by the barcode, engraved on the base of the sample holder. The scheme is very similar to the sample handling systems used at the Diamond protein crystallography (MX) beamlines. The robot system is interlocked to the safety system. The alignment procedure and the tomographic reconstruction is automated, using tailor-made software for alignment and the Diamond SAVU data pipeline for reconstruction[17].

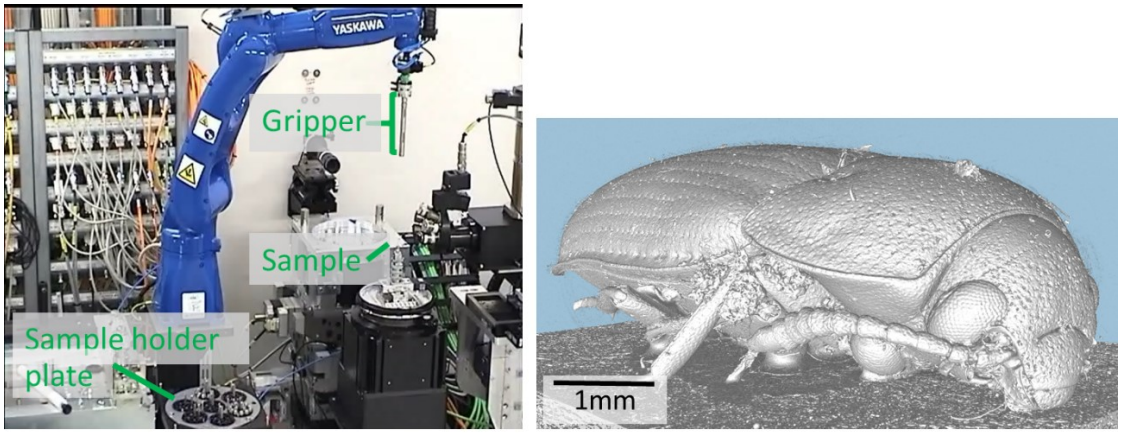

Figure 3: left: Sample changing robotic arm; right: example of surface rendered Mycetophagidae (hairy fungus beetle: sample courtesy A. Goswami, National History Museum London).

Up to 300 samples can be scanned per day. It allows exploring for example parameter space in materials with variable composition and preparation. Figure 3 right shows an application for life sciences in the area of bio-diversity (collaboration A. Goswami, NHM, London). Insects represent over a million known species and the development and evolution of this diversity is a central question. Phenotype encompasses morphology, development, physiology, and behavior and is the interface between an organism and their environment, including other individuals. Information on phenotype is critical for understanding how species evolve and respond to change, which is important in today's rapidly evolving environment. The current data acquisition and analyses capabilities will be improved further in terms of samples to be scanned and the automation of data analyses and requires a significant investment in data infrastructure.

3.1.2 Operando imaging

Operando imaging is typically performed with a large variety of sample environments, including heating, cooling, chemical reactors, rigs studying for example strain displacements below 100nm load[3] (see also references in[18]). Many experiments are carried out with the in-line phase contrast geometry, but apply also to other techniques. For increased sensitivity the

(single-) grating interferometry setup is used[19-24], which is compatible not only with the energy bandwidth provided by the multilayer monochromator but also in pink beam mode[10, 11]. Grating interferometry provides in addition phase and small angle scattering information. The phase signal is much more sensitive compared to the absorption and eases segmentation of data. Small angle scattering scales with electron density fluctuations and might help identifying the early stages of phase separation/transition occurring in materials[6]. As an example for operando imaging, the different processes for phase transition in anti-solvent transition is shown in figure 4. The picture on the left side shows the experimental setup including the reactor. At the tip of an inner and an outer tube, an anti-solvent is mixed with a solution, inducing a large variety of crystallization processes, see figure 4 (right). The technique will be improved and upgraded for a faster, more sensitive and detailed study and a better understanding of these processes, see also comments for the Diamond II upgrade including figure 6.

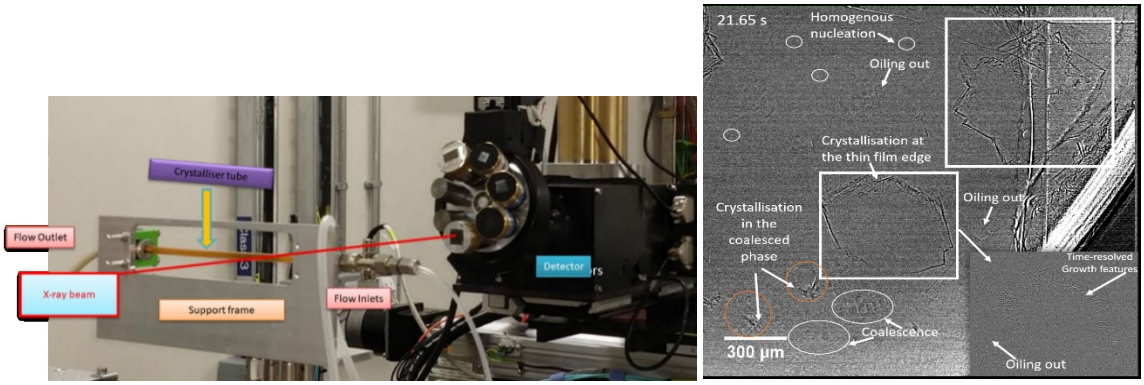

Figure 4: Operando imaging with dedicated sample environment /chemical reactor; left: experimental setup for crystallization studies induced by anti-solvent; right: different crystallization processes occurring in the mixing zone.

3.1.3 Fast Nano-tomography

For nano-imaging with 100nm resolution and below several methods are available on the imaging and coherence branch. While the timescales for the full-field microscope (TXM) are comparable to the other direct imaging methods, imaging in reciprocal space is significantly slower (see table 1).

The transmission X-ray microscope (TXM), located on the imaging branch, is using diffractive optics. The condenser optic is a so-called beam shaper[25], creating an illumination of 50-100 µm side length with the option of illumination of Zernike phase contrast (see references [9, 26] and also [27, 28]). The Fresnel-zone plate objective lenses provide a resolution of about 50-100 nm spatial resolution. For fast imaging using the multilayer monochromator the energy bandwidth is $\Delta E/E=10^{-3}$. Tomographic scans are typically recorded within minutes and has the potential to be reduced to the sub-minute to second regime by further optimising the setup and for specific cases, using machine learning algorithms[9].

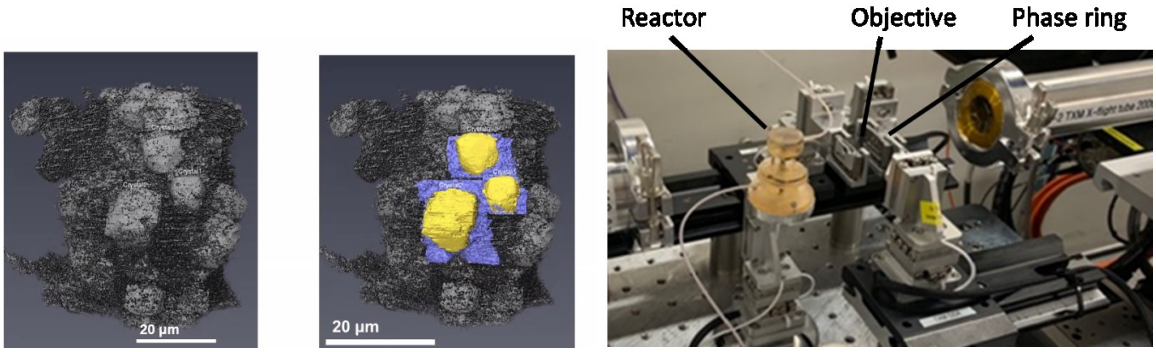

Figure 5: left and center: Deterioration of a 40 µm -thick X65 steel pin in a CO_2 saturated brine solution, heated at 80 ºC. The formation of an oxide scale and a localized corrosion site can be observed. Siderite crystals are formed, shown in yellow;

right: TXM with dedicated sample environment, here an in-situ flow cell, to study corrosion as a function of temperature, solution chemistry, and exposure time. All images courtesy Brian Connolly, Manchester University.

For the methods operating in reciprocal space (ptychography, Bragg-CDI), 3D data can be currently recorded within a couple of hours. For ptychography data acquisition with pink beam[29-31] and a data rate of up to 10kHz[31] have been demonstrated. Today a typical data acquisition rate is 800 Hz in fly-scan mode, scanning 200 $\mu m^2 s^{-1}$. For this reason temporal evolving structures can be studied in 2D, time series for tomographic studies can be achieved for any 'frozen' systems, where it is possible to interrupt and halt processes. Figure 6 shows a typical example for this kind of studies, investigating the crack propagation within a battery electrode[32]. The mechanical degradation of a $LiNi_{0.8}Co_{0.1}Mn_{0.1}O_2$ (NMC) cathode by Li+ cycling was performed by cycling the sample in-situ, halting the process and scanning the sample over 12 hours.

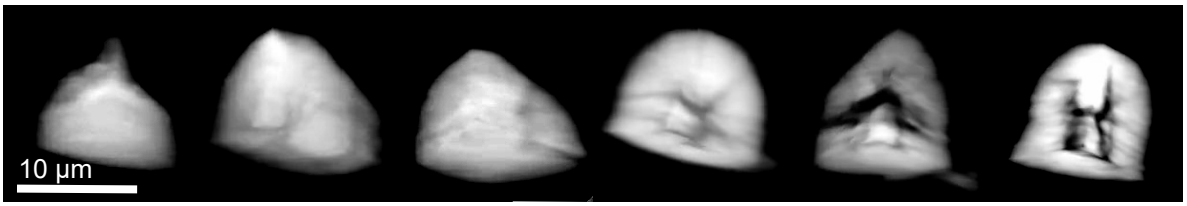

Figure 6: Formation of cracks within battery cathode material (NMC) along cycling process, recorded with ptychographic tomography[32].

4. OCTOPI: Diamond upgrade

In 2027 Diamond will undergo a major upgrades. They consist of increasing the storage ring energy from 3 to 3.5GeV, the reduction of the emittance by a factor of 20, new insertion devices and instrumentation upgrades. The I13 project OCTOPI '*Operando Computed TOmographic & Ptychographic Imaging'* will provide access to higher photon energies up to 40keV for micro-tomography, the further development of high-throughput & operando imaging also under cryo-conditions mainly for biological applications. While for micro-tomography a reduction of about 10x in recording times is expected, for nano-imaging the factor will be about hundred times (see figure 7, left). The slope of recording times versus length scale is significantly reduced with the impact that multiscale imaging with compatible recording times, e.g. similar number of samples, is enabled. Figure 7 right illustrates the impact on the accessible new science for the example of studying crystallisation, compare also figure 4.

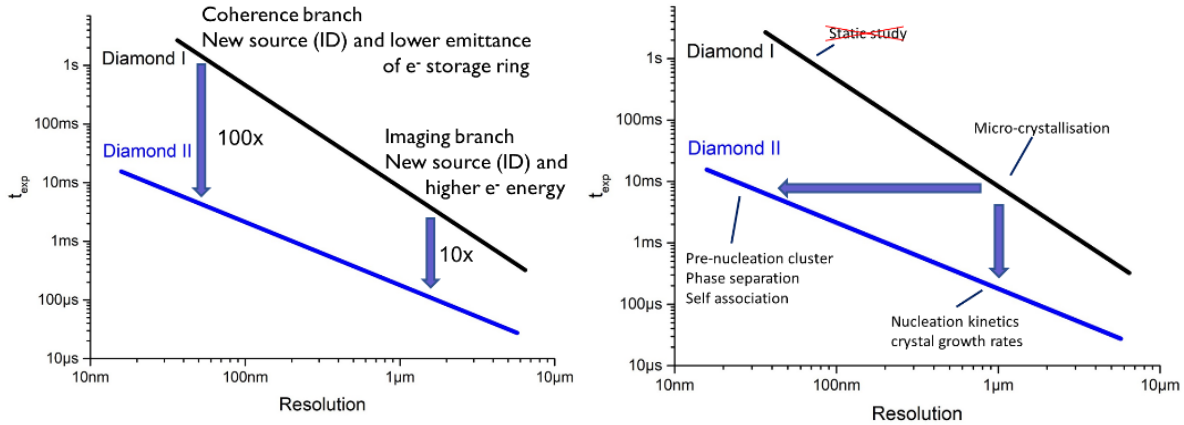

Figure 7: Diamond II upgrade impact on performance (left) and science (right), operando imaging of crystallization.

It will be possible to observe nucleation kinetics and crystal growth rates on the micrometer length scale, while with resolution in the 10nm range and time range of some ms the formation of pre-nucleation cluster, early stages of phase separation and the self-association of nucleation cores.

The beamline performs science in operando with micrometer to 100nm resolution and in-situ experiments for highest resolution. We explore several scientific areas currently, figure 8 illustrates the example for energy storage materials. The results are about the degradation of batteries such as the formation of dendrites in Zn electrodes, the formation of dendrites and the degradation of single NMC particles[32].With the Diamond II upgrade operando studies will be accessible across all length scales for a specific single system and scientific question.

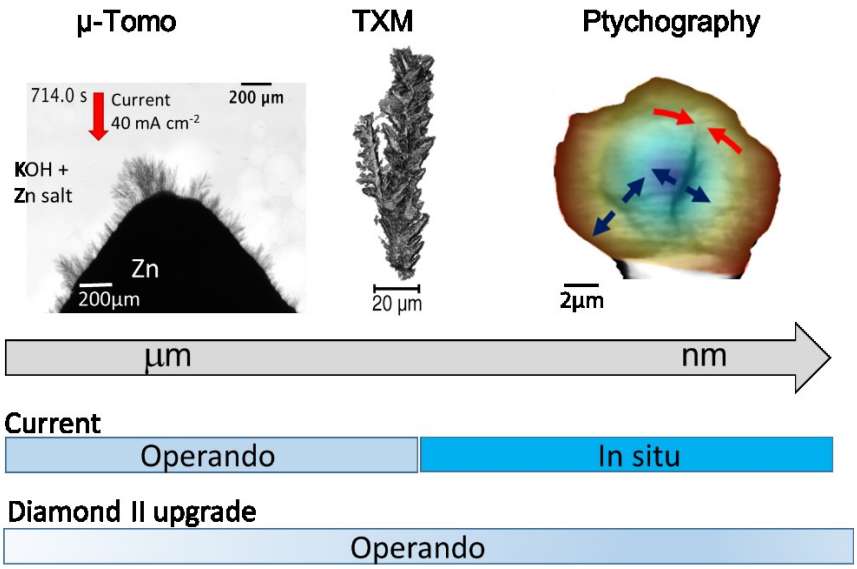

Figure 8: typical applications for energy storage materials from left to right: dendrite growth in Zn electrodes[33], zoom into a single dendrite, crack formation in battery cathode NMC particle[32].

5. SUMMARY

The beamline I13L provides imaging capabilities across different length scales for high sample throughput or imaging of processes. Key for most methods is the use of pink beam or a multilayer monochromator, increasing the effective photon flux by up to two orders of magnitude. Today operando tomography is available for processes on the minute/hour timescale and 2D imaging with milli- to micro-second time resolution. For highest spatial resolution below 100nm a single 3D scan takes hours currently and is suitable imaging series of 'frozen' systems.

In future this gap will be closed by the Diamond II upgrade, which will be beneficial in particular for the methods with highest spatial resolution (reciprocal space).

ACKNOWLEDGEMENTS

The authors especially thanks the teams of S.L.M. Schroeder (U. Leeds), J. Sefcik (U. Strathclyde), P. Shearing (UCL), A. Goswami (NHM) and B. Connolly (Manchester Univ.) for their contributions and sharing the results of their work. A. Korsunsky and P. Quinn are acknowledged for support and discussions. The Diamond-Manchester collaboration is acknowledged as well as the BP-ICAM/EPSRC Prosperity Partnership (EP/R00496X/1). The I13 team closely collaborates with C. David (PSI) and Florian Döring (XRnanotech) for X-ray optics. Kaz Wanelik and Huw Shorthouse provide excellent support for beamline controls and data acquisition. The use of laboratory facilities available at the Research Complex at Harwell and with financial support from the Future Continuous Manufacturing and Advanced Crystallization (CMAC) Hub (EPSRC Grant EP/P006965/1) and for G. Das a PhD studentship from the University of Leeds are acknowledged.

REFERENCES

[1] Singh, K., Menke, H., Andrew, M., Rau, C., Bijeljic, B., and Blunt, M. J., "Timeresolved synchrotron X-ray micro-tomography datasets of drainage and imbibition in carbonate rocks," Scientific Data, 5, (2018).

[2] Street, S. R., Xu, W., Amri, M., Guo, L., Glanvill, S. J. M., Quinn, P. D., Mosselmans, J. F. W., Vila-Comamala, J., Rau, C., Rayment, T., and Davenport, A. J., "The Effect of Nitrate on Salt Layers in Pitting Corrosion of 304L Stainless Steel," Journal of The Electrochemical Society, 162(9), C457-C464 (2015).

[3] Madi, K., Staines, K. A., Bay, B. K., Javaheri, B., Geng, H., Bodey, A. J., Cartmell, S., Pitsillides, A. A., and Lee, P. D., "In situ characterization of nanoscale strains in loaded whole joints via synchrotron X-ray tomography," Nature Biomedical Engineering, (2019).

[4] Barr, M. R., Jervis, R., Zhang, Y., Bodey, A. J., Rau, C., Shearing, P. R., Brett, D. J. L., Titirici, M. M., and Volpe, R., "Towards a mechanistic understanding of particle shrinkage during biomass pyrolysis via synchrotron X-ray microtomography and in-situ radiography," Scientific Reports, 11(1), 2656 (2021).

[5] Besnard, C., Harper, R. A., Moxham, T. E. J., James, J. D., Storm, M., Salvati, E., Landini, G., Shelton, R. M., and Korsunsky, A. M., "3D analysis of enamel demineralisation in human dental caries using high-resolution, large field of view synchrotron X-ray micro-computed tomography," Materials Today Communications, 27, 102418 (2021).

[6] Rau, C., Storm, M., Marathe, S., Bodey, A. J., Cipiccia, S., Batey, D., Shi, X. W., Zdora, M. C., and Zanette, I., [Multi-Scale Imaging at the Diamond Beamline I13], (2019).

[7] Rau, C., Wagner, U., Pesic, Z., and De Fanis, A., "Coherent imaging at the Diamond beamline I13," Physica Status Solidi a-Applications and Materials Science, 208(11), 2522-2525 (2011).

[8] Rau, C., "Imaging with Coherent Synchrotron Radiation: X-ray Imaging and Coherence Beamline (I13) at Diamond Light Source," Synchrotron Radiation News, 30(5), 19-25 (2017).

[9] Storm, M., Döring, F., Marathe, S., David, C., and Rau, C., "The Diamond I13 full-field transmission X-ray microscope: a Zernike phase-contrast setup for material sciences," Powder Diffraction, 35(S1), S8-S14 (2020).

[10] Marathe, S., Storm, M., Kuppili, S. C., Harrison, R., Das, G., Schroeder, S. L. M., Cipiccia, S., Döring, F., David, C., and Rau, C., "Development of synchrotron pink beam X-ray grating interferometer for fast imaging and tomography applications," 11113, 1111319 (2019).

[11] Marathe, S., Das, G., Schroeder, S. L. M., Ziesche, R., Baird, E., and Rau, C., "High-speed grating interferometery."

[12] Rau, C., Weitkamp, T., Snigirev, A., Schroer, C., Benner, B., Tummler, J., Gunzler, T., Kuhlmann, M., Lengeler, B., Krill, C., Doebrich, K., Michels, D., and Michels, A., "Tomography with high resolution," Proceedings of the SPIE, 4503, 14-22 (2002).

[13] Rack, A., Morawe, C., Mancini, L., Dreossi, D., Parkinson, D. Y., Mac Dowell, A. A., Siewert, F., Rack, T., Holz, T., Kramer, M., and Dietsch, R., "Reflection on multilayer mirrors: beam profile and coherence properties," Proceedings of SPIE, 9207, 92070V (2014).

[14] Rack, A., Vivo, A., Helfen, L., and Morawe, C., "Beam profile and coherence properties of synchrotron beams after reflection on modified multilayer mirrors," AIP Conference Proceedings, 1741, 040026 (2016).

[15] Storm, M., Döring, F., Marathe, S., Cipiccia, S., David, C., and Rau, C., "Optimizing the energy bandwidth for transmission full-field X-ray microscopy experiments " Journal of Synchrotron Radiation, submitted.

[16] Disney, C. M., Madi, K., Bodey, A. J., Lee, P. D., Hoyland, J. A., and Sherratt, M. J., "Visualising the 3D microstructure of stained and native intervertebral discs using X-ray microtomography," Scientific Reports, 7(1), 16279 (2017).

[17] Atwood, R. C., Bodey, A. J., Price, S. W. T., Basham, M., and Drakopoulos, M., "A high-throughput system for high-quality tomographic reconstruction of large datasets at Diamond Light Source," Philos. Trans. R. Soc. Ser. A, 373(2043), 20140398 (2015).

[18] Rau, C., Bodey, A., Storm, M., Cipiccia, S., Marathe, S., Zdora, M. C., Zanette, I., Wagner, U., Batey, D., and Shi, X., "Micro- and Nano-Tomography at the DIAMOND beamline I13L Imaging and Coherence," Proceedings of SPIE, 10391(2017).

[19] Momose, A., Kawamoto, S., Koyama, I., Hamaishi, Y., Takai, K., and Suzuki, Y., "Demonstration of X-Ray Talbot interferometry," Japanese Journal of Applied Physics Part 2-Letters & Express Letters, 42(7B), L866-L868 (2003).

[20] Weitkamp, T., Diaz, A., David, C., Pfeiffer, F., Stampanoni, M., Cloetens, P., and Ziegler, E., "X-ray phase imaging with a grating interferometer," Optics Express, 13(16), 6296-6304 (2005).

[21] Zdora, M. C., Vila-Comamala, J., Schulz, G., Khimchenko, A., Hipp, A., Cook, A. C., Dilg, D., David, C., Grunzweig, C., Rau, C., Thibault, P., and Zanette, I., "X-ray phase microtomography with a single grating for high-throughput investigations of biological tissue," Biomedical Optics Express, 8(2), 1257-1270 (2017).

[22] Marathe, S., Zdora, M. C., Zanette, I., Cipiccia, S., and Rau, C., "Comparison of Data Processing Techniques for Single Grating X-ray Talbot Interferometer Data," Proceedings of SPIE, 10391, 103910S (2017).
[23] Bikis, C., Rodgers, G., Deyhle, H., Thalmann, P., Hipp, A., Beckmann, F., Weitkamp, T., Theocharis, S., Rau, C., Schulz, G., and Muller, B., "Sensitivity comparison of absorption and grating-based phase tomography of paraffin-embedded human brain tissue," Applied Physics Letters, 114(8), 083702 (2019).
[24] Rodgers, G., Schulz, G., Deyhle, H., Marathe, S., Bikis, C., Weitkamp, T., and Muller, B., "A quantitative correction for phase wrapping artifacts in hard X-ray grating interferometry," Applied Physics Letters, 113(9), 093702 (2018).
[25] Jefimovs, K., Vila-Comamala, J., Stampanoni, M., Kaulich, B., and David, C., "Beam-shaping condenser lenses for full-field transmission X-ray microscopy," Journal of Synchrotron Radiation, 15, 106-108 (2008).
[26] Storm, M., Cipiccia, S., Marathe, S., Kuppili, V. S. C., Doring, F., David, C., and Rau, C., "The Diamond I13-2 Transmission X-ray Microscope: Current Status and Future Developments," Microscopy and Microanalysis, 24(S2), 216-217 (2018).
[27] Vila-Comamala, J., Bosgra, J., Eastwood, D. S., Wagner, U., Bodey, A. J., Garcia-Fernandez, M., David, C., and Rau, C., "Transmission X-ray Microscopy at Diamond-Manchester I13 Imaging Branchline," AIP Conference Proceedings, 1696, 020036 (2016).
[28] Stampanoni, M., Mokso, R., Marone, F., Vila-Comamala, J., Gorelick, S., Trtik, P., Jefimovs, K., and David, C., "Phase-contrast tomography at the nanoscale using hard x rays," Physical Review B, 81(14), 140105(R) (2010).
[29] Edo, T. B., Batey, D. J., Maiden, A. M., Rau, C., Wagner, U., Pesic, Z. D., Waigh, T. A., and Rodenburg, J. M., "Sampling in x-ray ptychography," Physical Review A, 87(5), 053850 (2013).
[30] Batey, D. J., Edo, T. B., Rau, C., Wagner, U., Pesic, Z. D., Waigh, T. A., and Rodenburg, J. M., "Reciprocal-space up-sampling from real-space over sampling in x-ray ptychography," Physical Review A, 89(4), 043812 (2014).
[31] Cipiccia, S., Batey, D., Shi, X., Williams, S., Wanelik, K., Wilson, A., Martin, P., Scott, T., and Rau, C., "Multi-scale multi-dimensional imaging at I13-coherence branchline in Diamond Light Source," AIP Conference Proceedings, 2054, 050005 (2019).
[32] Romano Brandt, L., Marie, J.-J., Moxham, T., Förstermann, D. P., Salvati, E., Besnard, C., Papadaki, C., Wang, Z., Bruce, P. G., and Korsunsky, A. M., "Synchrotron X-ray quantitative evaluation of transient deformation and damage phenomena in a single nickel-rich cathode particle," Energy & Environmental Science, 13(10), 3556-3566 (2020).
[33] Yufit, V., Tariq, F., Eastwood, D. S., Biton, M., Wu, B., Lee, P. D., and Brandon, N. P., "Operando Visualization and Multi-scale Tomography Studies of Dendrite Formation and Dissolution in Zinc Batteries," Joule, 3(2), 485-502 (2019).